Analysis of I-V-T characteristics of Be-doped AlGaAs Schottky diodes grown on (100) GaAs substrates by Molecular Beam Epitaxy

Slimane Oussalah[1,*], Walid Filali[2], Elyes Garoudja[2], Boumediene Zatout[1], Fouaz Lekoui[3], Rachid Amrani[4,5], Noureddine Sengouga[6] and Mohamed Henini[7]

[1] *Division Microélectronique et Nanotechnologies, Centre de Développement des Technologies Avancées, cité 20 août 1956, Baba Hassen, 16081 Alger, Algeria*

[2] *Plateforme Technologique de Microfabrication, Centre de Développement des Technologies Avancées, cité 20 août 1956, Baba Hassen, 16081 Alger, Algeria*

[3] *Division Milieux Ionisés et Laser, Centre de Développement des Technologies Avancées, cité 20 août 1956, Baba Hassen, 16081 Alger, Algeria*

[4] *Département des Sciences de la Matière, Université Benyoucef Benkhedda Alger 1, Alger, Algeria*

[5] *LPCMME, Département de physique, Université d'Oran ES-Sénia, Oran, Algérie*

[6] *Laboratory of Metallic and Semiconducting Materials (LMSM), Université Mohamed Khider Biskra, BP 145 RP, 07000 Biskra, Algeria*

[7] *School of Physics and Astronomy, University of Nottingham, Nottingham, NG7 2RD, UK*

*Corresponding author: soussalah@cdta.dz

Abstract

The temperature effect on the electrical characteristics of Au/Ti on Beryllium-doped $Al_{0.29}Ga_{0.71}As$ Schottky diodes grown on (100) GaAs substrates by molecular beam epitaxy has been investigated for various temperatures ranging from 260 to 400 K. By assuming thermionic emission is the dominant mechanism by which carrier transport occurs in Schottky barriers, the forward and reverse current–voltage ($I-V$) characteristics are analyzed to assess the main Schottky diode electronic parameters, such as ideality factor (n) , barrier height ($\emptyset_B$), series resistance (R_S) and saturation current (I_S). These parameters are extracted by using different approaches, such as the conventional $I-V$ method, Cheung and Cheung's method and Norde's method. The $I-V$ analysis showed an abnormal behavior, namely an increase of $\emptyset_B$ and a decrease of n with increasing temperature. This strong dependence of Schottky diode parameters with temperature was attributed to the spatial inhomogeneity at the metal-semiconductor (MS) interface. By assuming a Gaussian distribution of the barrier heights at the MS interface, the inhomogeneity of the barrier height has been successfully explained. In addition, the temperature dependent energy distribution of interface states density (N_{SS}) profiles was obtained from the forward bias I–V measurements by taking into account the bias dependence of the effective barrier height ($\emptyset_e$) and n.

Keywords: AlGaAs, Gaussian distribution, heterostructure, inhomogeneous Schottky barrier height, temperature effect.

1. Introduction

Gallium Arsenide (GaAs)-based structures are amongst the most familiar and investigated III-V compound semiconductors because of their wide field of applications, such as optoelectronics, photovoltaics, and high-frequency and low power devices [1-5]. This is due to their remarkable physical properties such as direct energy bandgap and high electron mobility. Aluminium Gallium Arsenide ($Al_xGa_{1-x}As$), which is lattice matched to GaAs, has a larger bandgap than GaAs and is widely used as an active material in many heterostructures for a wide range of device applications, such as high electron mobility transistors [6], lasers [7], particle detectors [8] and Schottky barrier diodes (SBDs) [9, 10]. SBD is a metal-semiconductor (MS) contact that exhibits a rectified current–voltage ($I-V$) characteristic. The fabrication of Schottky contacts must be well controlled to ensure reliable operation of the device. Thereby, the MS interface characterization is very important [11].

The graphical representation analysis of SBDs $I-V$ measurements at only room temperature does not provide enough information to understand their conduction mechanism or the barrier formation nature at the MS interface. Therefore, $I-V$ as well as capacitance–voltage ($C-V$) measurements as a function of temperature are commonly used in order to obtain a detailed explanation of the different aspects of the conduction mechanisms through the MS contacts. These measurement techniques permit the extraction of the main electronic parameters of the Schottky diode such as the contact barrier height ($\emptyset_B$), the ideality factor (n), the saturation current (I_S), the series resistance (R_S), and the density of surface states (N_{ss}) [12].

Based on the thermionic emission theory (TE), several approaches were adopted in the literature to extract the SBD electronic parameters, among them $I-V$ method [13], Cheung and Cheung method [14] and Norde method [15]. These methods have shown their great aptitude to determine these parameters in question.

In this work, p-type AlGaAs Schottky diodes grown on (100) semi-insulating GaAs substrates by Molecular Beam Epitaxy (MBE) have been fabricated using Ti/Au metallization as Schottky contact. $I-V$ characteristics were measured in a temperature range of 260-400 K using the methods cited above in the goal to extract the Schottky barrier electronic parameters and give an explanation to the observed effects. $I-V$ characteristics show a strong temperature dependency of n and $\emptyset_B$. By increasing temperature, $\emptyset_B$ increases and n decreases. This dependency reveals the presence of a Gaussian distribution of inhomogeneous barrier heights in the Schottky diodes [16]. Additionally, N_{ss} as a function of energy distribution was determined from the forward $I - V$ characteristics by taking into account the bias dependence of the effective barrier height.

The remainder of this paper is structured as follows. Section 2 gives the device fabrication experimental details and characterization tools used. The discussion of the obtained results is given in Section 3. Finally, the last section provides concluding remarks.

2. **Experimental details**

The molecular beam epitaxy (MBE) technique was used to fabricate p-type beryllium doped $Al_{0.29}Ga_{0.71}As$ based Schottky diodes on semi-insulating (100) GaAs substrates [17]. Fig. 1(a) and Fig. 1(b) show a schematic diagram of the structure and a scanning electron microscope (SEM) image of top Schottky contact, respectively. The device structure consists of 0.45 μm undoped GaAs buffer layer followed by 1 μm of Be-doped $Al_{0.29}Ga_{0.71}As$ epitaxial layer. The Be-doping concentration is about 10^{+16} cm^{-3}. Different Schottky contact diameters (250, 300, 400, 600, 800, 1000 μm) were elaborated by evaporating Titanium/Gold (Ti/Au) on the top of the epitaxial layer. The bottom Ohmic contact to the doped AlGaAs layer was obtained by chemical etching and depositing Gold/Nickel/Gold (Au/Ni/Au) which were annealed at a temperature of 360°C in H2/Ar mixture as shown in Fig. 1(a). The fabricated samples were mounted in a Janis CCS-450 helium closed-cycle refrigerator system where temperature was controlled with a LakeShore 331S cryogenic temperature controller. The $(I - V)$ measurements of Schottky diodes were performed with Keithley 238 source-measure unit (SMU). A personal computer has been programmed to control the measurement bench and record the data thanks to the LabVIEW software tool.

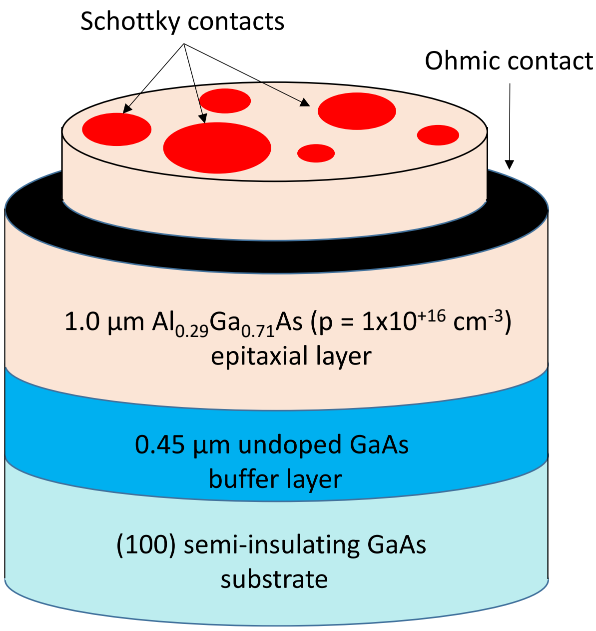

(a)

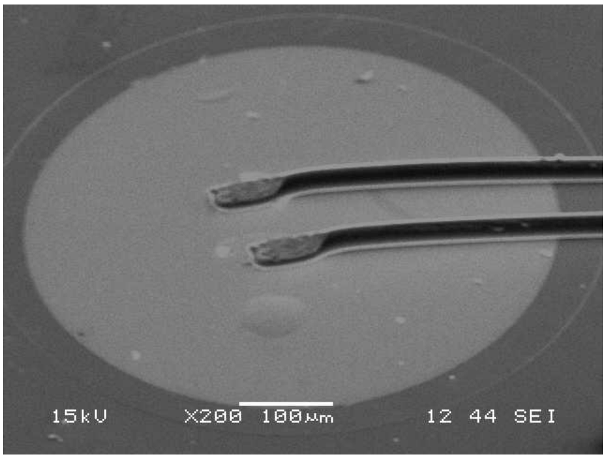

(b)

Figure 1**.** (a) Schematic layer structure of the Be-doped $Al_{0.29}Ga_{0.71}As$ Schottky diode. (b) SEM image of top Schottky contact with a diameter of 800 µm.

3. **Results and discussions**

3.1.Temperature dependence of $I - V$ characteristics

The forward and reverse ($I - V$) characteristics of the Schottky diode on a semi-logarithmic scale measured at different temperatures ranging from 260 to 400 K are shown in Fig. 2. As clearly seen, the diodes show a good rectifying behavior. At the low-bias region (0.1 - 0.3 V), the current rises rapidly with increasing bias voltage, while it slows down enormously for voltages higher than 0.4 V. As can one see, $I - V$ characteristics have the usual form in the first region of the plot while in the second region, it clearly indicated the appearance of the series resistance effect and the activation of the interface states within the band gap when the applied voltage moves away from the low-bias region. On the other side, for the reverse bias condition, the current increases gradually with the voltage bias. The non-saturation of the current is due to several effects such as tunneling, image force, existence of traps and interface states [18].

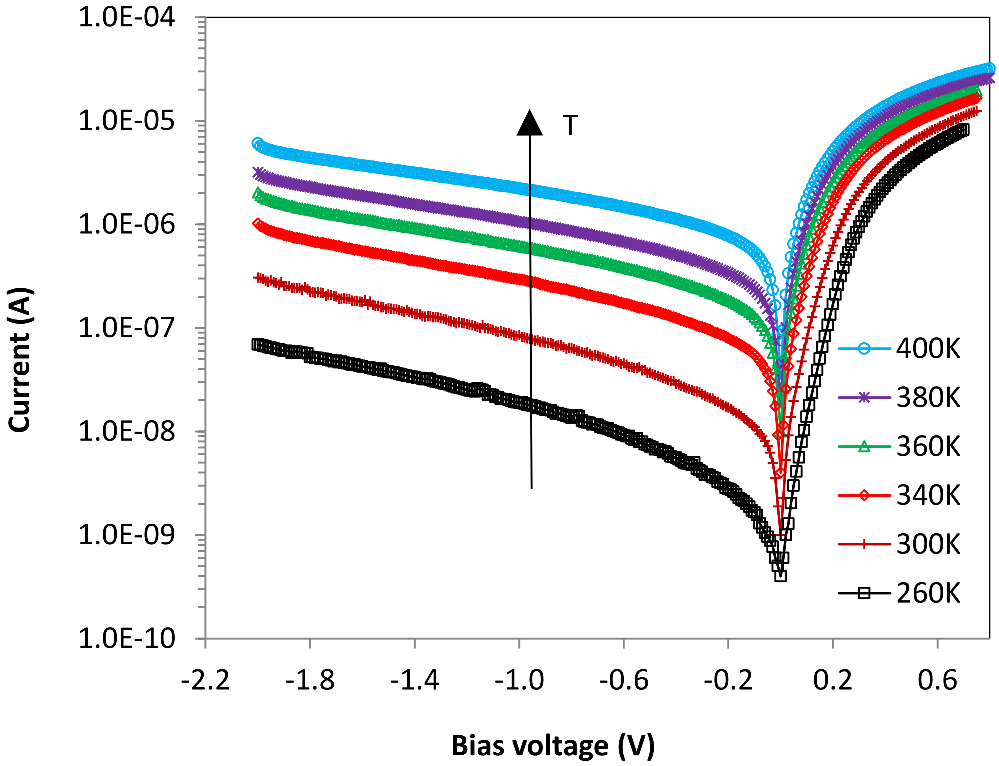

Figure 2. Experimental forward and reverse $I - V$ curves of the Au/Ti/p-type AlGaAs SBDs for temperatures ranging from 260 to 400 K.

Figure 3 shows the rectifying ratio (I_F/I_R) variation with temperature at an applied voltage of 0.5 V. I_F/I_R is obtained by dividing the forward current to the reverse current. As can be seen I_F/I_R decreases exponentially as temperature increases. At room temperature I_F/I_R is about 170 as compared to 1480 for a similar sample but grown on (311)A GaAs substrate with a same doping concentration [19]. The plausible reason for the higher reverse current for sample grown on (100) can be explained by the higher trap concentrations as compared to (311)A GaAs orientation as indicated in the references [20, 21].

The increase in the reverse current (leakage current) at high temperature is the main reason of the degradation of the diodes rectification.

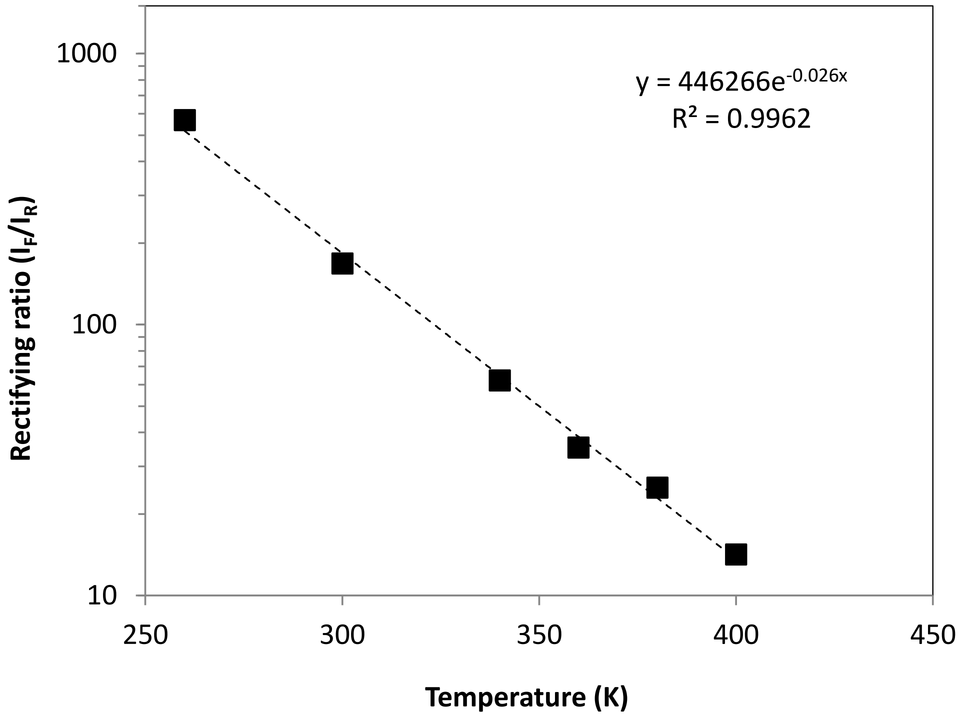

Figure 3. Rectifying ratio of the Au/Ti/ p-type AlGaAs SBDs for temperatures ranging from 260 to 400 K.

When the diode is biased at a voltage V higher than $3kT/q$, the current flow through the barrier of the MS contact with the presence of series resistance, obeys the thermionic emission (TE) mechanism [13] according to the equation (1).

$$I(V) = I_S\left[\exp\left(\frac{V-R_S I}{nV_T}\right) - 1\right] \tag{1}$$

where $V_T = kT/q$ is the thermal voltage and k, T, and q, are the Boltzmann's constant , the absolute temperature in Kelvin , and the electron charge, respectively. n can be derived from the linear region slope of $\ln(I) - V$ plot using the relation:

$$n = \frac{1}{V_T}\frac{dV}{d(\ln(I))} \tag{2}$$

The voltage $V - R_S I$ across the diode can be represented as the overall voltage drop across the diode plus its series resistance. The intercept of $\ln(I)$ at zero bias voltage gives I_S that is expressed by:

$$I_S = AA^*T^2 \exp\left(\frac{-\emptyset_{B0}}{V_T}\right) \qquad (3)$$

where the quantities A, $\emptyset_{B0}$, A^*, are the rectifier contact area of the MS diode, the apparent BH at zero bias, and the effective Richardson constant ($A^* = 56.8\ Acm^{-2}K^{-2}$ for p-type AlGaAs) [22, 23], respectively. The basic assumption of the TE model is that the electrons have to go over the barrier in order to cross the boundary between the metal and the semiconductor. The knowledge of $\emptyset_{B0}$, n, R_S and I_S will help understand the conduction mechanism in the Schottky barrier diode. For this purpose, different methods are used to extract these electronic parameters from experimental $I - V$ characteristics.

Knowing I_S and $\emptyset_{B0}$ determined from Eq. (3), R_S can be calculated from Eq. (1). R_S can also be determined from the deviation of the $\log(I) - V$ curve from linearity at high currents according to the expression $\Delta V = R_S I$ [12].

For $R_S I < V$, Eq. (1) can be rewritten as [24, 25]:

$$I(V) = I_S exp\left(\frac{V}{nV_T}\right)\left[1 - exp\left(\frac{V}{V_T}\right)\right] \qquad (4)$$

The plot of $log\left[I/\left(1 - exp(-V/V_T)\right)\right]$ versus V using Eq. (4) should be linear all the way to $V = 0$, except for a series resistance effect over the high current density portion of the data. $\emptyset_{B0}$, n, and I_S are extracted in the same manner as from Eq. (1).

The $I - V$ characteristics of the Au/Ti/p-AlGaAs SBD are non-linear at high forward bias, as illustrated in Fig.2, which may be attributed to the effect of R_S and N_{SS} at the MS interface.

The values of R_S as well as those of $\emptyset_{B0}$ and n, can also be determined from the non-linear region of the forward bias $I-V$ characteristics using a method developed by Cheung and Cheung [14]. Cheung's functions can be written as follows:

$$\frac{dV}{d(ln(I))} = R_S I + nV_T \tag{5}$$

$$H(I) = V - nV_T ln\left(\frac{I}{AA^*T^2}\right) \tag{6}$$

After some simplification steps, $H(I)$ function will be given as follow:

$$H(I) = R_S I + n\emptyset_{B0} \tag{7}$$

In the downward-curvature region of the forward bias I-V characteristics, Eq. (5) should yield a straight line. As a result, $\mathrm{dV/dln}(I)$ vs I plot yields R_S as a slope and n as the y-axis intercept. On the other hand, the slope of $H(I)$ vs I plot (Eq. (7)) gives another determination of R_S and $\emptyset_{B0}$. If R_S values obtained from Eq. (5) and Eq. (7) are almost equal, this implies that Cheung's method is consistent. The plots of $\mathrm{dV/dln}(I)$ and $H(I)$ as a function of I at room temperature for the studied samples are shown in Fig. 4.

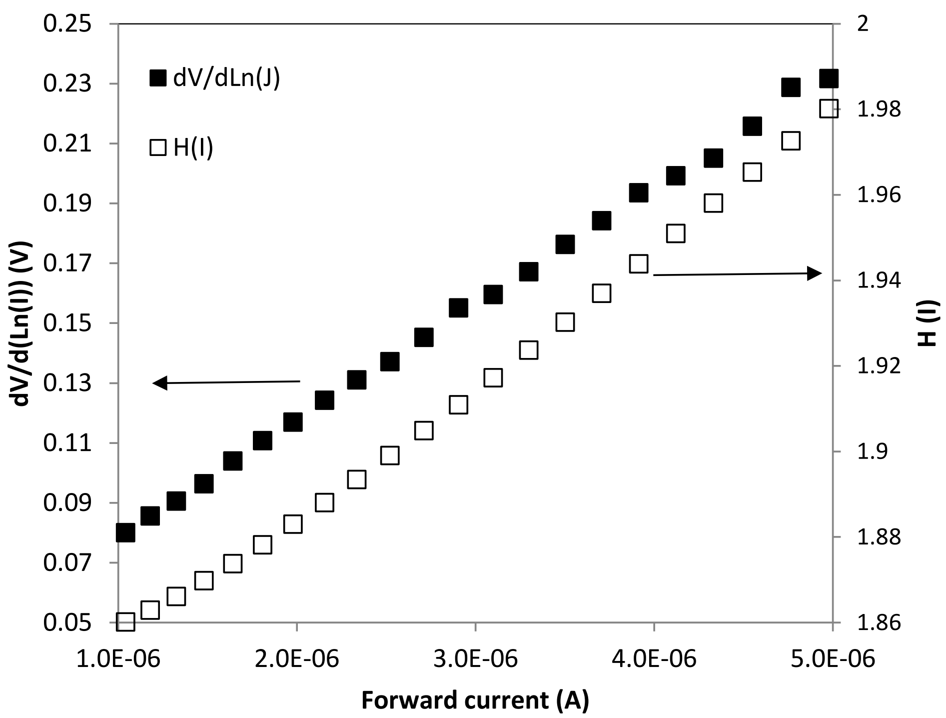

Figure 4. $\mathrm{dV}/\mathrm{dln}(I)$ vs I and $H(I)$ vs I plots of the Au/Ti/p-type AlGaAs SBDs at room temperature.

An alternative extraction method was developed by Norde [15] in order to determine the diode parameters. Norde proposed that even in the presence of series resistance, a reliable value of $\emptyset_{B0}$ can be derived. Norde's function $F(V)$ is given by:

$$F(V) = \frac{V}{\gamma} - V_T \ln\left(\frac{I(V)}{AA^*T^2}\right) \tag{8}$$

where γ is a dimensionless integer greater than n. V and $I(V)$ are voltage and current obtained from the $I - V$ measurements. First, $F(V)$ vs V plot is determined, as shown in Fig. 5, then $\emptyset_{B0}$ can be derived from Eq. (9):

$$\emptyset_B = F(V_0) + \frac{V_0}{\gamma} - V_T \tag{9}$$

where $F(V_0)$ represents the minimum value of $F(V)$ of the plot $F(V)$ vs V, and V_0 is the corresponding voltage. R_S can be estimated from the Norde's function as [15] :

$$R_S = \frac{\gamma - n}{I_0} V_T \quad (10)$$

where I_0 is the current that corresponds to V_0.

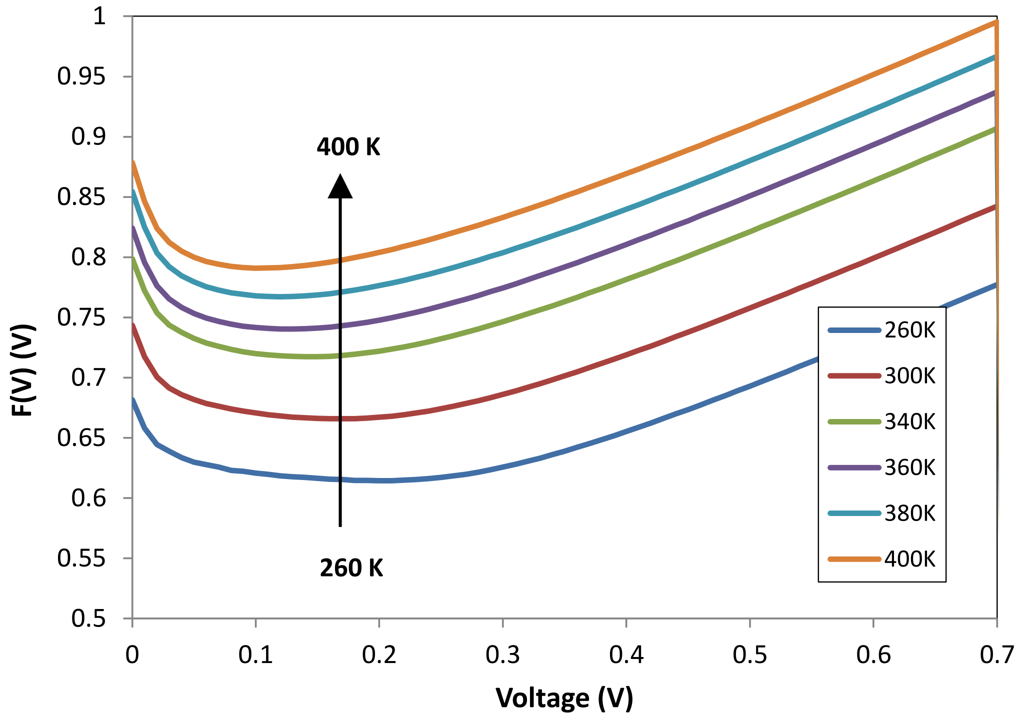

Figure 5. Calculated plots of $F(V)$ vs V at different temperatures of the Au/Ti/p-type AlGaAs SBDs for temperatures ranging from 260 to 400 K.

In addition to the SBD parameters extraction methods mentioned above, $\emptyset_{B0}$ can also be extracted from the reverse $I - V$ plots [11, 25-26]. As shown in Fig. 6, a plot of $log\left[I/\left(1 - exp(-V/V_T)\right)\right]$ as a function of reverse bias voltage yields I_S from the intercept of the linear region of the curve at zero bias. Once I_S is determined, $\emptyset_{B0}$ can be obtained using Eq. (2), thus:

$$\emptyset_{B0} = V_T \ln\left(\frac{AA^*T^2}{I_S}\right) \tag{11}$$

In theory, n and $\emptyset_{B0}$ extracted from ideal $I-V$ characteristics driven by pure TE should be temperature independent. Figure 2 shows non-ideal $I-V$ characteristics of Au/Ti/p-type AlGaAs Schottky diodes indicating a departure from pure TE theory. The experimental values of n and $\emptyset_{B0}$ were determined from different extraction methods at different temperatures, as illustrated in Figs. 7 and 8, respectively.

As can one seen in Fig. 7, n values are higher than unity and exhibit a decreasing trend with increasing temperature. These values can be ascribed to various effects such as the existence of interfacial insulator layer at MS interface, distribution of interface states within the semiconductor band gap, tunneling effect, recombination-generation of carriers, image-force barrier lowering effect, and barrier inhomogeneities [16, 27-31].

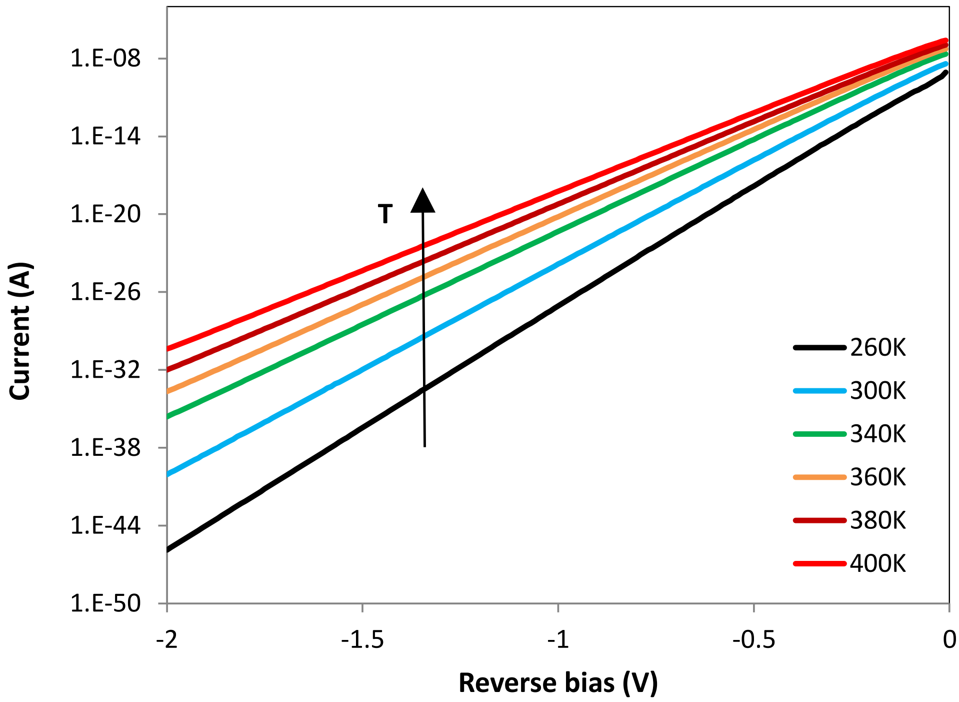

Figure 6. Plot of semi-logarithmic $I/\left(1-exp(-V/V_T)\right)$ versus reverse bias voltage of the Au/Ti/p-type AlGaAs SBDs for temperatures ranging from 260 to 400 K.

Contrary to ideality factor, the value of zero-bias BH ($\emptyset_{B0}$), which is calculated from different extraction methods, shows an unexpected tendency, namely an increase in value with increasing temperature (Fig. 8). Such temperature dependence contradicts the stated negative temperature coefficient of the GaAs barrier height [32, 33]. As explained in [34, 35], charge carriers at low temperatures may overcome the lower barriers because current transport across the MS interface is a temperature activated process. Hence, current transport will be dominated by current flowing through patches with lower BHs and a higher ideality factor. As the temperature increases, more and more charge carriers have enough energy to overcome the higher barrier. As a result, the dominant barrier height will increase with the temperature and the bias voltage [29, 36, 37] .

In the temperature range of 260–400 K, we can see that there is a barrier height difference of 0.06–0.09 eV between forward and reverse bias. This difference is acceptable as reported in literature [26, 38, 39]. The values of $\emptyset_{B0}$ determined by Norde's method are nearly identical to those determined with the standard model, while Cheung's method exhibits higher extracted values of $\emptyset_{B0}$. This could be due to the fact that Cheung's method is applied to only the nonlinear region of the forward $I - V$ characteristics with higher bias voltage.

As seen in Fig. (9), R_S values increase with decreasing temperature. As temperature decreases, R_S values determined using Cheung's method are, closer to those determined using the standard method, whereas R_S values extracted using Norde's method exhibit higher values.

This could be because Cheung's method only applies to the nonlinear region of the forward $I - V$ characteristics at higher bias, whereas Norde's method applies to the complete forward bias $I - V$ characteristics. Furthermore, Norde's method may not be suitable for Schottky diodes with high ideality factors, which are incompatible with the pure TE mechanism [40, 41].

Figure 10 shows the extracted saturation current from the forward and reverse characteristics. As can we see, the values obtained from forward characteristics differ by a factor of two from those obtained from reverse ones. This may be due to the fitting processes. In both cases I_S decreases with decreasing temperature that is to be expected because I_S is related to the free carrier intrinsic density, which increases with temperature.

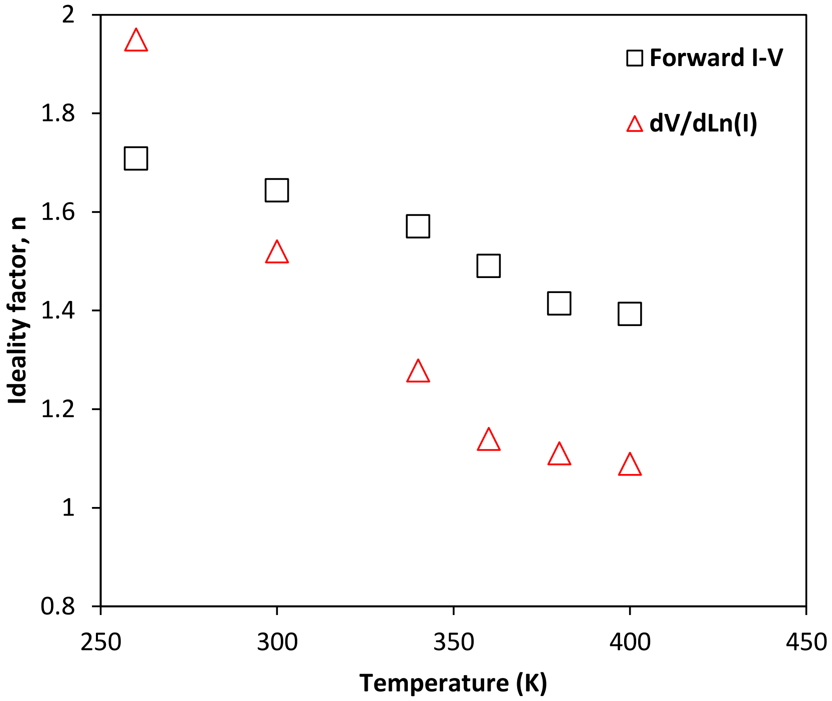

Figure 7. Temperature dependence of ideality factor n extracted from forward I-V curves and Cheung methods of Au/Ti/p-type AlGaAs SBDs.

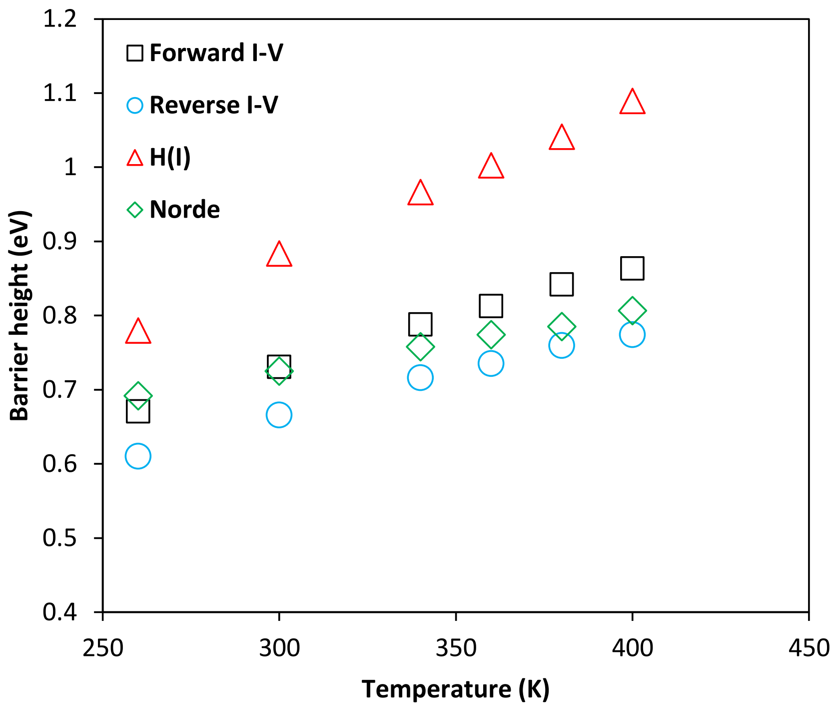

Figure 8. Temperature dependence of barrier height $\emptyset_{B0}$ extracted from different methods of Au/Ti/p-type AlGaAs SBDs.

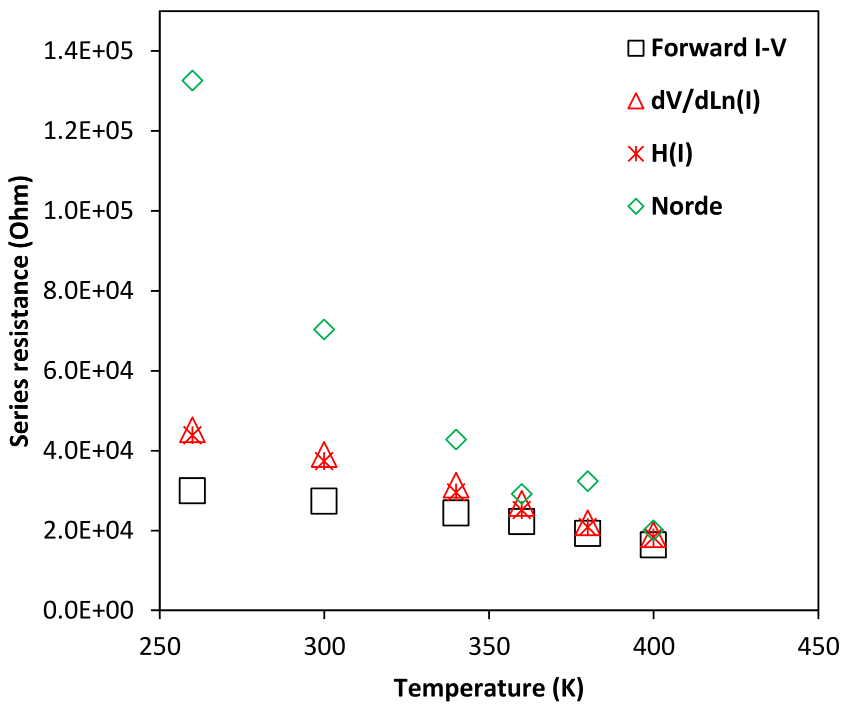

Figure 9. Temperature dependence of series resistance extracted from different methods of Au/Ti/p-type AlGaAs SBDs.

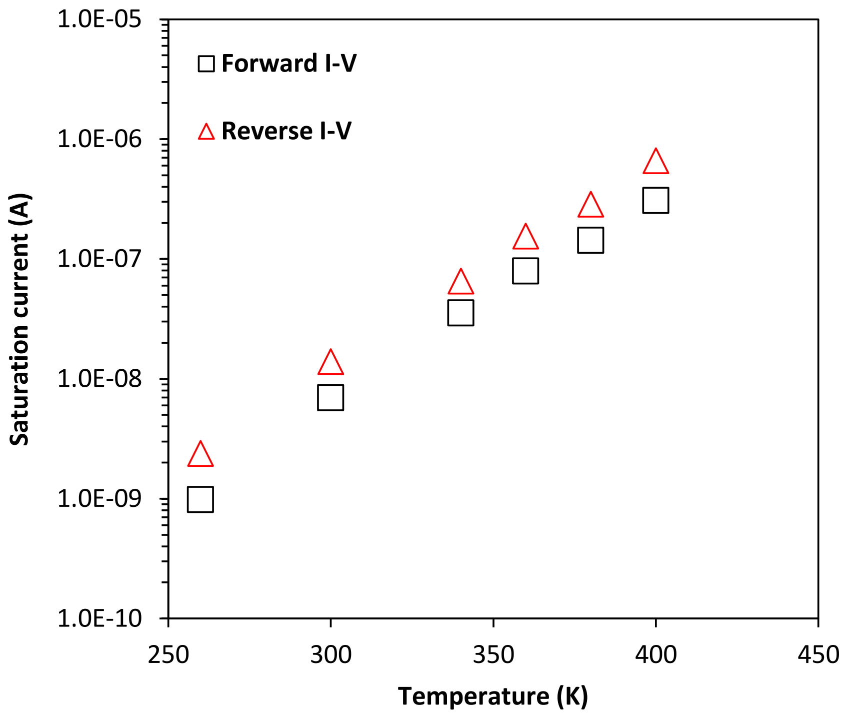

Figure 10. Temperature dependence of saturation current extracted from forward and reverse I-V curves of Au/Ti/p-type AlGaAs SBDs.

As can be seen, the values of SBD parameters extracted from experimental I–V data are strongly depending on the method used. This is due to the fact that each method is applied to the whole forward bias region (Norde method), non-linear region (Cheung method) or linear region (conventional I-V method). We think that Cheung method exhibits some advantages by its simplicity, which offers the possibility to extract device parameters at each temperature, and has the ability to perform for high resistance and non-ideal devices. If we assume the conventional I-V method as the reference method, Norde methods lose their reliability at low temperatures, as can be seen for series resistance. Furthermore, the difficulty in the determination of minimum points of F(V) vs V plots is still a problem can cause this inconsistency.

The ideality factors determined from the slope of the $I - V$ curves linear region take into account some effects, some of which are related to the interfacial parameters that make the device to be non-ideal. In addition, voltage-dependent ideality factor $n(V)$ can be calculated using Eq. (1) as follows:

$$n(V) = \frac{1}{V_T}\frac{V}{\ln(I/I_S)} \tag{12}$$

Moreover, the energy dependent value (E_{SS}) of interface states density (N_{SS}) in p-type semiconductors with regard to the top of the valence band (E_V) at the semiconductor surface is given by [27, 42]:

$$E_{ss} - E_V = q(\Phi_e - V) \tag{13}$$

where $\emptyset_e$ is the effective BH that can be calculated from Eq. (14) [42-44] :

$$\emptyset_e = \emptyset_{B0} + \left(1 - \frac{1}{n(V)}\right)V \tag{14}$$

The thin interfacial layer between the metal and the semiconductor is considered to be homogeneous and has distinct effects on the MS contact behavior [27, 43]. Card and Rhoderick proposed that the ideality factor becomes greater than unity for a real Schottky diodes where all of the interface states are in equilibrium with the semiconductor [27], and is given by:

$$n(V) = 1 + \frac{d}{\varepsilon_i}\left[\frac{\varepsilon_s}{W_D} + qN_{ss}(V)\right] \tag{15}$$

This expression is the same as Card and Rhoderick Eq. (18) [27] and the interface state density can be written as :

$$N_{ss}(V) = \frac{1}{q}\left[\frac{\varepsilon_i}{d}(n(V) - 1) - \frac{\varepsilon_s}{W_D}\right] \tag{16}$$

where d is the interfacial layer thickness estimated to be 30-40 Ǻ [27, 45, 46] and W_D is the depletion layer width obtained from experimental $C - V$ characteristics at 1 MHz [22]. ε_i=3.5ε_0 [13, 29] and ε_S=12.4ε_0 are the interfacial insulator layer and the semiconductor permittivity, respectively, where ε_0 is the free space.

At each temperature, the values of the voltage dependence of $n(V)$ calculated from the $I - V$ data shown in Fig. 2 are substituted in Eq. (12). N_{SS} values were determined from Eq. (16) as a function of $(E_{SS} - E_V)$ and are presented in Fig. 11. As can one see from Fig. 11, the interface state density increases from mid-gap towards the top of valence band, which indicates the continuum of the interface states. N_{SS} values are quite high and of the order 10^{+13} $eV^{-1}cm^{-2}$ and decrease with increasing temperature. Temperature's effect on interface states is most likely due to thermal restructuring and reordering of the MS interface [43].

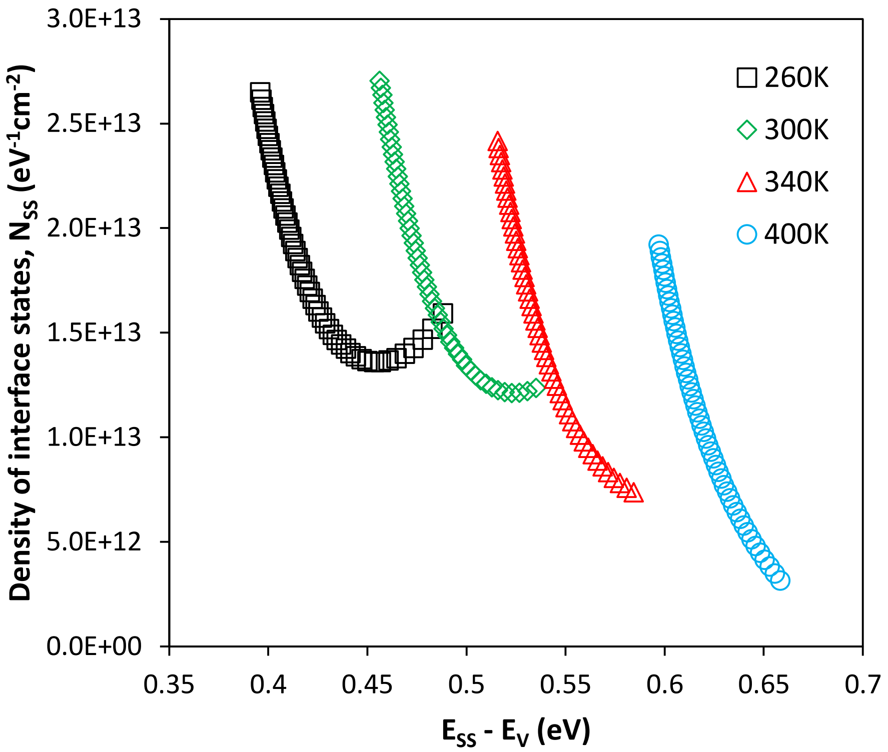

Figure. 11. Distribution of the interface state density (N_{SS}) in the band gap of Au/Ti/p-type AlGaAs SBDs for different temperatures.

3.2. Analysis of the abnormal variation of n and $\emptyset_{B0}$ with temperature

For further investigation of the non-ideal behavior of the forward bias $I - V$ characteristics, we obtained the conventional activation energy (E_a) by transforming Eq. (3) to the so-called Richardson plot, as given by Eq. 17:

$$ln\left(\frac{I_S}{T^2}\right) = ln(AA^*) - \frac{1000}{T}\emptyset_{B0} \quad (17)$$

According to Eq.17, the plot of ln I_S/T^2 versus 1000/T (Figure 12) gives a straight line with a slope given by the activation energy (E_a) at 0 K, and the intercept at the ordinate given by the Richardson constant (A^*). It results in $E_a = 0.31$ eV and $A^* = 4.64 \times 10^{-6}$ $Acm^{-2}K^{-2}$. The E_a value is very small compared to the energy band gap of AlGaAs at 300 K (E_g=1.8 eV). Because the Richardson plot activation energy represents the effective BH, this observation confirms that TE is not the major conduction mechanism.

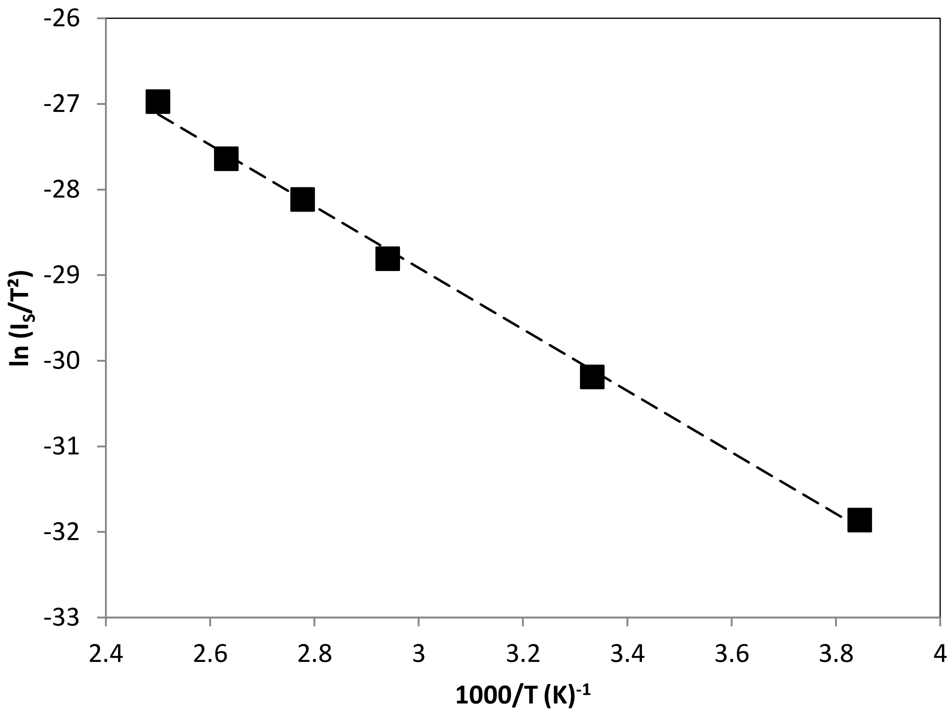

Figure .12. The Richardson plot of $\ln(I_S/T^2)$ versus $1000/T$ of Au/Ti/p-type AlGaAs SBDs.

Additionally, A^* is much lower than the theoretical value of 56.8 $Acm^{-2}K^{-2}$ for p-type AlGaAs [22, 23]. The unrealistic value of the A^* is commonly attributed to the spatial inhomogeneous barrier height and potential fluctuation at the MS interface which consists of low and high barrier areas, i.e. the current flows preferentially via the lower barrier in the potential distribution. To address this issue, Werner and Güttler [16] proposed an inhomogeneous Gaussian spatial distribution of the BH modeled by a function giving the probability of barrier height occurrence, expressed by:

$$P(\emptyset_B) = \frac{1}{\sigma\sqrt{2\pi}} exp\left(-\frac{\left(\emptyset_B - \overline{\emptyset}_B\right)^2}{2\sigma^2}\right) \tag{18}$$

where $\overline{\emptyset}_B$ and σ are the mean value of the BH and the standard deviation, respectively. The pre-exponential term $1/\sigma\sqrt{2\pi}$ is used to represent constant value for normalizing the Gaussian BH distribution. The parameters $\overline{\emptyset}_B$ and σ are assumed to vary linearly with bias as follows:

$$\overline{\emptyset}_B = \overline{\emptyset}_{B0} + \gamma V \tag{19}$$

$$\sigma = \sigma_0 + \xi V \tag{20}$$

where $\overline{\emptyset}_{B0}$ and σ_0 are zero-bias reference values, and γ and ξ are temperature-independent coefficients that model the barrier distribution's voltage deformation. The temperature dependency of σ is usually small and may be neglected [16]. As a result, the total current across the MS contact at a forward bias containing barrier inhomogeneities can be expressed as:

$$I(V) = \int_{-\infty}^{+\infty} I(\emptyset_B, V)\, P(\emptyset_B) d\emptyset_B \tag{21}$$

where $I(\emptyset_B, V)$ is the current component corresponding to the barrier height $\emptyset_B$ at a voltage bias V based on the TE model. By introducing $I(\emptyset_B, V)$ and $P(\emptyset_B)$ from Eqs. (1) and (19) into Eq. (21) and performing the integration within the limits $-\infty$ and $+\infty$, we obtain [16]:

$$I(V) = I_S \left[exp\left(\frac{V - R_S I}{n_{ap} V_T}\right) - 1\right] \quad (22)$$

where

$$I_S = AA^* T^2 exp\left(-\frac{\emptyset_{Bap}}{V_T}\right) \quad (23)$$

$\emptyset_{Bap}$ and n_{ap} represent the apparent Schottky BH and apparent ideality factor, respectively, and are given by:

$$\emptyset_{Bap}(T) = \overline{\emptyset}_{B0} - \frac{\sigma_0^2}{2V_T} \quad (24)$$

$$\frac{1}{n_{ap}(T)} - 1 = -\gamma + \frac{\xi}{2V_T} \quad (25)$$

To characterize the Schottky barrier inhomogeneity, both $\emptyset_{Bap}$ and n_{ap} are plotted versus $1/2V_T$ as illustrated in Fig. 13. The plot shown in Fig.13 is a straight line and conform to the inhomogeneous Schottky diode model proposed by Werner and Güttler [16]. The linear best fit of $\emptyset_{Bap}$ gives $\overline{\emptyset}_{B0} = 1.214$ eV and $\sigma_0 = 160$ mV from the slope.

It is worth noting that $\overline{\emptyset}_{B0}$ is slightly greater than the uniform value determined previously, and σ_0 that represents the Schottky barrier inhomogeneity, is not negligible. Indeed, a lower σ_0 indicates a more homogeneous SBH.

The linear behavior of $1/n - 1$ vs $1/2V_T$ plot shown in Fig. 13 proves that n obtained from $I - V$ curves of Schottky diodes represents the voltage deformation of the barrier distribution at the inhomogeneous interface [16]. From this plot we determined the coefficient $\gamma = 0.0429$ from the intercept and $\xi = -13.5$ mV from the straight-line slope.

As previously stated, A* is determined from the conventional $\ln I_S/T^2$ vs $1000/T$ plot and it is value is much lower than the theoretical one. To explain this abnormal behavior, the modified Richardson plot can be obtained by combining Eqs. 23 and 24, which lead to the following expression:

$$ln\left(\frac{I_S}{T^2}\right) - \frac{1}{2}\left(\frac{\sigma_0}{V_T}\right)^2 = ln(AA^*) - \frac{\bar{\emptyset}_{B0}}{V_T} \qquad (26)$$

The modified Richardson plot is illustrated in Fig. 14. According to Eq. (26), the plot of $[ln(I_s/T^2) - (\sigma_0^2/2V_T^2)/2]$ versus $1/V_T$ should be linear with a slope that yields the mean barrier height $\bar{\emptyset}_{B0}$ and the intercept on the ordinate that directly yields the effective Richardson constant A^*. The least squares method is used to find the slope and the intercept of the $[ln(I_S/T^2) - (\sigma_0^2/2V_T^2)/2]$ versus $1/V_T$ plot that allowed the determination of $\bar{\emptyset}_{B0} = 1.21\ eV$ and $A^* = 58.6\ Acm^{-2}K^{-2}$. It is worth noting that the modified Richardson constant is in accordance with the expected theoretical value of $56.8\ \ Acm^{-2}K^{-2}$. We can conclude that the abnormal behavior of the Schottky diode with temperature is due to the inhomogeneous distribution of the barrier height [47, 48].

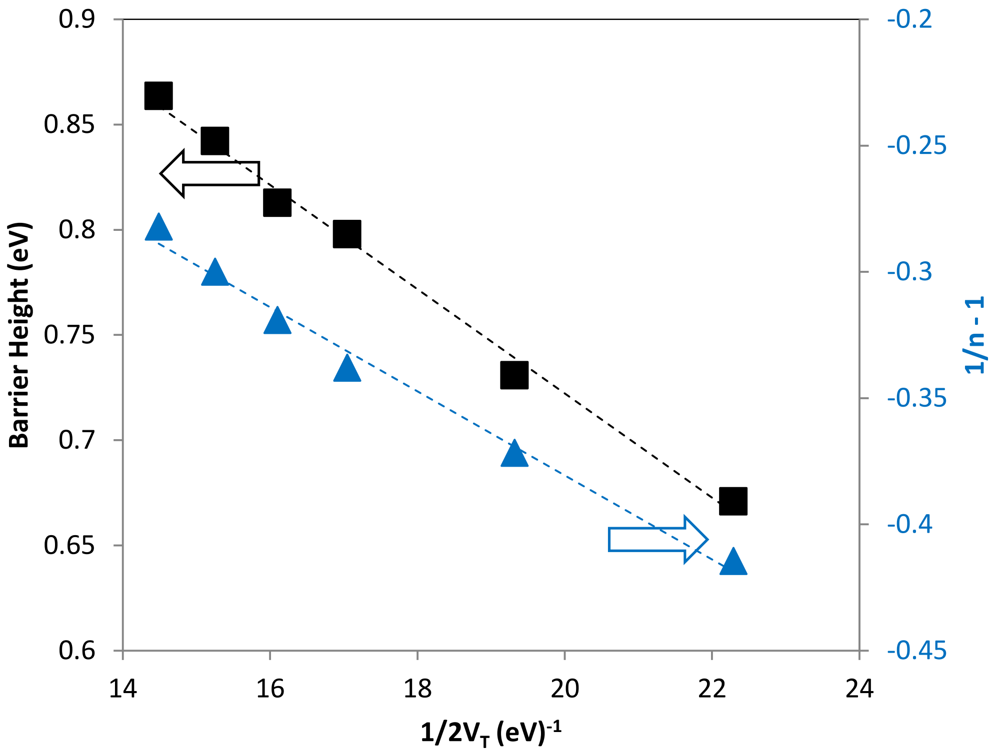

Figure .13. Apparent zero-bias BH $(\emptyset_{Bapp})$ and $\left({}^{1}/_{n} - 1\right)$ versus $1/2V_T$ plots of Au/Ti/p-type AlGaAs SBDs according to a Gaussian distribution of BHs.

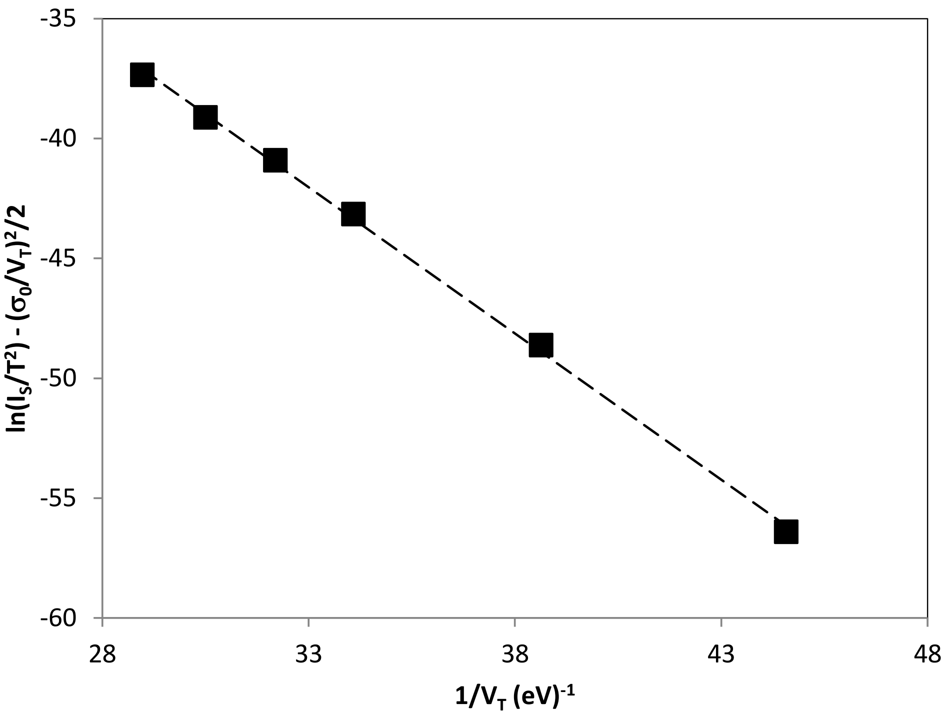

Figure.14. The modified Richardson $\ln(I_0/T^2) - (\sigma_0/2V_T)^2$ versus $1/V_T$ plot of Au/Ti/p-type AlGaAs SBDs according to a Gaussian distribution of BHs.

Conclusion

In summary, p-type Beryllium-doped $Al_{0.29}Ga_{0.71}As$ Schottky diodes grown on (100) semi-insulating GaAs by Molecular Beam Epitaxy were investigated using forward and reverse $I-V$ characteristics for various temperatures in the range 260-400 K. Based on the thermionic emission mechanism, the main electronic parameters of the Schottky diode such as the ideality factor (n), the barrier height $(\emptyset_{B0})$, the series resistance (R_S) and the interface states density (N_{SS}) were extracted from standard $I-V$ characteristics, Cheung's method and Norde's method. These approaches allowed the understanding of carrier transport mechanism and interface properties of the studied metal-semiconductor structure.

A linear relation of the rectifying ratio (forward current/reverse current) as a function of temperature was observed. The energy distribution profile of interface states density (N_{SS}) was obtained from the forward bias I–V characteristics at various temperatures, by taking into account the effective barrier height ($\emptyset_e$) bias dependence of Au/Ti/p-type AlGaAs Schottky diodes. N_{SS} values were quite high varying from $3x10^{+12}$ to $3x10^{+13}$ $eV^{-1}cm^{-2}$, however they decreases when the temperature increases. From the experimental $I - V$ characteristics, the extracted electrical parameters from different methods, showed a decrease in Schottky barrier height, from 1.1 to 0.6 eV, and an increase in ideality factor, from 1.1 to 1.9, with decreasing temperature. This abnormal behaviour was successfully explained by assuming a Gaussian distribution of the lateral Schottky barrier height inhomogeneities. Based on this assumption, a modified Richardson plot given by $[\ln(I_S/T^2) - (\sigma_0/V_T)^2/2]$ versus V_T(equal to kT/q) was obtained. It is seen that the zero bias standard deviation value σ_0 (0.16 eV) is not small compared to the mean value of the barrier height $\overline{\emptyset}_{B0}$, which is 1.21 eV, indicating large inhomogeneities at the interface and hence potential fluctuations. The effective Richardson constant value was found to be 58.6 $Acm^{-2}K^{-2}$ from the modified Richardson plot, which is very close to the theoretical value of 56.8 $Acm^{-2}K^{-2}$ for p-type AlGaAs given in literature.

References

[1] S. Mokkapati and C. Jagadish, III-V compound SC for optoelectronic devices, Mater. Today 12 (2009), pp. 22-32.

[2] S. S. Li, High-Speed III–V Semiconductor Devices, in Semiconductor Physical Electronics, Springer, New York, 2006.

[3] O. Wada, Optoelectronic integration based on GaAs material, Opt. Quantum Electron. 20 (1988), pp. 441-474.

[4] J. Yoon, S. Jo, I. S. Chun, I. Jung, H. Kim, M. Meitl, E. Menard, X. Li, J. J. Coleman, U. Paik, and J. A. Rogers, GaAs photovoltaics and optoelectronics using releasable multilayer epitaxial assemblies, Nature 465 (2010), pp. 329-333.

[5] F. Schwierz and J. J. Liou, RF transistors: Recent developments and roadmap toward terahertz applications, Solid-State Electron. 51 (2007), pp. 1079-1091.

[6] L. A. Tracy, J. L. Reno, S. Fallahi, and M. J. Manfra, Integrated high electron mobility transistors in GaAs/AlGaAs heterostructures for amplification at sub-Kelvin temperatures, Appl. Phys. Lett. 114 (2019), pp. 053104-1-053104-5.

[7] P. Zhang, C. Liu, M. Xiang, X. Ma, G. Zhao, Q. Lu, J. F. Donegan, and W. Guo, 850 nm GaAs/AlGaAs DFB lasers with shallow surface gratings and oxide aperture, Opt. Express 27 (2019), pp. 31225-31234.

[8] A. A. Marmalyuk, M. A. Ladugin, A. Y. Andreev, K. Y. Telegin, I. V. Yarotskaya, A. S. Meshkov, V. P. Konyaev, S. M. Sapozhnikov, E. I. Lebedeva, V. A. Simakov, AlGaAs/GaAs laser diode bars (λ= 808 nm) with improved thermal stability, Quantum Electron. 43 (2013), p. 895.

[9] J. E. Lees, A. M. Barnett, D. J. Bassford, J. S. Ng, C. R. Tan, J. P. R. David, N. Babazadeh, R. B. Gomes, P. Vines, R. D. McKeag, and D. Boe, Development of AlGaAs avalanche diodes for soft X-ray photon counting, IEEE NSS Conference Record, Valencia, 2011, p. 4528.

[10] F. Mustafa, N. Parimon, A. M. Hashim, S. F. Abd Rahman, A. R. A. Rahman, and M. N. Osman, Design, fabrication and characterization of a Schottky diode on an AlGaAs/GaAs HEMT structure for on-chip RF power detection, Superlattices Microstruct. 47 (2010), pp. 274-287.

[11] W. Filali, N. Sengouga, S. Oussalah, R. H. Mari, D. Jameel, N. A. Al Saqri, M. Aziz, D. Taylor, and M. Henini, Characterisation of temperature dependent parameters of multi-

quantum well (MQW) Ti/Au/n-AlGaAs/n-GaAs/n-AlGaAs Schottky diodes, Superlattices Microstruct. 111 (2017), pp. 1010-1021.

[12] D. K. Schroder, Semiconductor material and device characterization: John Wiley & Sons, New York, 2015.

[13] S. Sze and K. K. Ng, Physics of Semiconductor Devices, John Wiley & Sons, New York, 1981.

[14] S. Cheung and N. Cheung, Extraction of Schottky diode parameters from forward current-voltage characteristics, Appl. Phys. Lett. 49 (1986), pp. 85-87.

[15] H. Norde, A modified forward I-V plot for Schottky diodes with high series resistance, J. Appl. Phys. 50 (1979), pp. 5052-5053.

[16] J. H. Werner and H. H. Güttler, Barrier inhomogeneities at Schottky contacts, J. Appl. Phys. 69 (1991), pp. 1522-1533.

[17] W. Filali, E. Garoudja, S. Oussalah, N. Sengouga, M. Henini, and D. Taylor, The Efficiency of Best-so-far ABC Algorithm Versus Analytical Methods for Schottky Diode Parameters Extraction, J. Nano- and Electronic physics 11 (2019), pp. 05012-1-05012-5, 2019.

[18] F. Padovani, The voltage–current characteristic of metal–semiconductor contacts, Semicond. and Semimet. 7 (1971), pp. 75-146.

[19] N. A. Al-Ahmadi, F. A. Ebrahim, H. A. Al-Jawhari, R. H. Mari, and M. Henini, Impact of doping on the performance of p-type Be-doped Al0. 29 Ga0. 71As Schottky diodes, Mod. Electron. Mater. 3 (2017), pp. 66-71.

[20] R.H Mari, "Electrical Characterisation of Defects in III-V Compound Semiconductors by DLTS", PhD thesis, University of Nottingham, 2011.

[21] R.H. Mari, M. Shafi, M.Aziz, A. Khatab, D. Taylor, M. Henini, “Electrical characterisation of deep level defects in Be-doped AlGaAs grown on (100) and (311)A GaAs substrates by MBE”, Nanoscale Research Letters 2011,6:180.

[22] S. Adachi, Physical properties of III-V semiconductor compounds: John Wiley & Sons, New York, 1992.

[23] Silvaco-TCAD, Atlas User’s Manual, Device Simulation Software, Silvaco Int., Santa Clara, CA, 2015.

[24] E. H. Rhoderick, Metal-semiconductor contacts, IEE Proc. I, Solid-State and Electron Devices, 129 (1982), pp. 1-14.

[25] J. Waldrop, Schottky-barrier height of ideal metal contacts to GaAs, Appl. Phys. Lett. 44 (1984), pp. 1002-1004.

[26] K. Zeghdar, L. Dehimi, A. Saadoune, and N. Sengouga, Inhomogeneous barrier height effect on the current–voltage characteristics of an Au/n-InP Schottky diode, J. Semicond. 36 (2015), p. 124002.

[27] H. Card and E. Rhoderick, Studies of tunnel MOS diodes I. Interface effects in silicon Schottky diodes, J. Phys. D: Appl. Phys. 4 (1971), p. 1589.

[28] Ş. Altındal, S. Karadeniz, N. Tuğluoğlu, and A. J. S.-S. E. Tataroğlu, The role of interface states and series resistance on the I–V and C–V characteristics in Al/SnO2/p-Si Schottky diodes, Solid-State Electron. 47 (2003), pp. 1847-1854.

[29] R. Tung, Electron transport of inhomogeneous Schottky barriers, Appl. Phys. Lett. 58 (1991), pp. 2821-2823.

[30] R. T. Tung, Formation of an electric dipole at metal-semiconductor interfaces, Phys. Rev. B 64 (2001), p. 205310.

[31] M. K. Hudait and S. Krupanidhi, Effects of thin oxide in metal–semiconductor and metal–insulator–semiconductor epi-GaAs Schottky diodes, Solid-State Electron. 44 (2000), pp. 1089-1097.

[32] M. Hudait, P. Venkateswarlu, and S. Krupanidhi, Electrical transport characteristics of Au/n-GaAs Schottky diodes on n-Ge at low temperatures, Solid-State Electron. 45 (2001), pp. 133-141.

[33] Ş. Altındal, H. Kanbur, D. Yıldız, and M. Parlak, Current conduction mechanism in Al/p-Si Schottky barrier diodes with native insulator layer at low temperatures, Appl. Surf. Sci. 253 (2007), pp. 5056-5061.

[34] R. Tung, J. Sullivan, and F. Schrey, On the inhomogeneity of Schottky barriers, Mater. Sci.Eng. B 14 (1992), pp. 266-280.

[35] J. P. Sullivan, R. Tung, M. Pinto, and W. J. J. o. a. p. Graham, Electron transport of inhomogeneous Schottky barriers: A numerical study, J. Appl. Phys. 70 (1991), pp. 7403-7424.

[36] A. Gümüş, A. Türüt, and N. Yalcin, Temperature dependent barrier characteristics of CrNiCo alloy Schottky contacts on n-type molecular-beam epitaxy GaAs, J. Appl. Phys. 91 (2002), pp. 245-250.

[37] Ş. Karataş, Ş. Altındal, A. Türüt, and A. Özmen, Temperature dependence of characteristic parameters of the H-terminated Sn/p-Si (1 0 0) Schottky contacts, Appl. Surf. Sci. 217 (2003), pp. 250-260.

[38] K. Çınar, N. Yıldırım, C. Coşkun, and A. Turut, Temperature dependence of current-voltage characteristics in highly doped Ag/p-GaN/In Schottky diodes, J. Appl. Phys. 106 (2009), p. 073717.

[39] K. Ejderha, A. Zengin, I. Orak, B. Tasyurek, T. Kilinc, and A. Turut, Dependence of characteristic diode parameters on sample temperature in Ni/epitaxy n-Si contacts, Mater. Sci. Semicond. Process. 14 (2011), pp. 5-12.

[40] P. S. Reddy, V. Janardhanam, I. Jyothi, C. S. Harsha, V. R. Reddy, S.-N. Lee, et al., Effect of copper phthalocyanine thickness on surface morphology, optical and electrical properties of Au/CuPc/n-Si heterojunction, Appl. Phys. A 124 (2018), pp. 1-10.

[41] V. Janardhanam, I. Jyothi, K.-S. Ahn, and C.-J. Choi, Temperature-dependent current–voltage characteristics of Se Schottky contact to n-type Ge, Thin Solid Films 546 (2013), pp. 63-68.

[42] A. Singh, K. Reinhardt, and W. Anderson, Temperature dependence of the electrical characteristics of Yb/p-InP tunnel metal-insulator-semiconductor junctions, J. Appl. Phys. 68 (1990), pp. 3475-3483.

[43] A. Bengi, S. Altındal, S. Özçelik, and T. Mammadov, Gaussian distribution of inhomogeneous barrier height in Al0. 24Ga0. 76As/GaAs structures, Physica B: Condensed Mat. 396 (2007), pp. 22-28.

[44] P. Cova and A. Singh, Temperature dependence of IV and CV characteristics of Ni/n-CdF2 Schottky barrier type diodes, Solid-State Electron. 33 (1990), pp. 11-19.

[45] A. Cowley and S. Sze, Surface states and barrier height of metal-semiconductor systems, J. Appl. Phys. 36 (1965), pp. 3212-3220.

[46] A. Tataroğlu and Ş. Altındal, Characterization of current–voltage (I–V) and capacitance–voltage–frequency (C–V–f) features of Al/SiO2/p-Si (MIS) Schottky diodes. Microelectron. Eng. 83 (2006), pp. 582-588.

[47] S. Asubay, A. Turut, A useful model to interpret the experimental I-V-T and C-V-T data of spatially inhomogeneous metal-semiconductor rectifying contacts, Australian Journal of Electrical and Electronics Engineering, 17(2020), pp. 278-285.

[48] I. Jabbari, M. Baira, H. Maaref, R. Mghaieth, Schottky barrier inhomogeneity in (Pd / Au) Al0.22 Ga0.78N/GaN/SiC HEMT: Triple Gaussian distributions, Chinese Journal of Physics, 73 (2021), pp. 719-731.